

Biophysical Journal, Volume 120

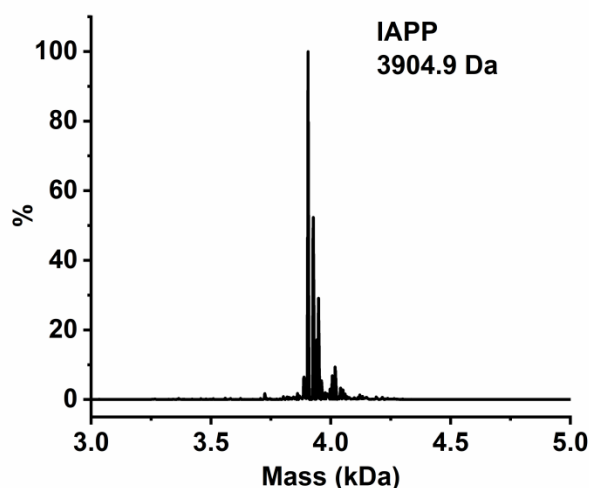
Supplemental Information

**Hsp70 Inhibits Aggregation of IAPP by Binding to the Heterogeneous
Prenucleation Oligomers**

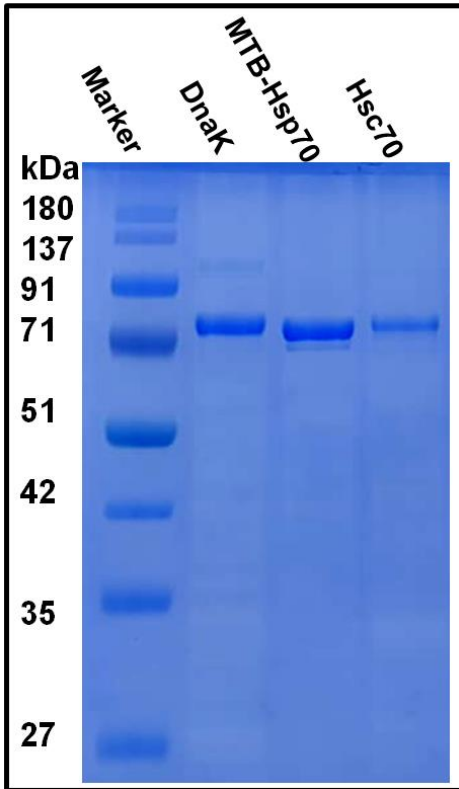
**Neeraja Chilukoti, Timir Baran Sil, Bankanidhi Sahoo, S. Deepa, Sreelakshmi
Cherakara, Mithun Maddheshiya, and Kanchan Garai**

Mass spectrometry of chemically synthesized purified IAPP

A 100 μ l of IAPP sample was injected into the HPLC fitted with reverse phase column (Advance Biopeptide map column, Agilent), which is connected inline with an ESI-MS mass spectrometer (Agilent technologies, UK). The m/z spectra were deconvoluted using the inbuilt program in the resolved isotope mode and mass of 3904.9 Da was noted for IAPP which is similar to that of the theoretical MW of IAPP containing disulphide bridge between 2 and 7 cysteine.



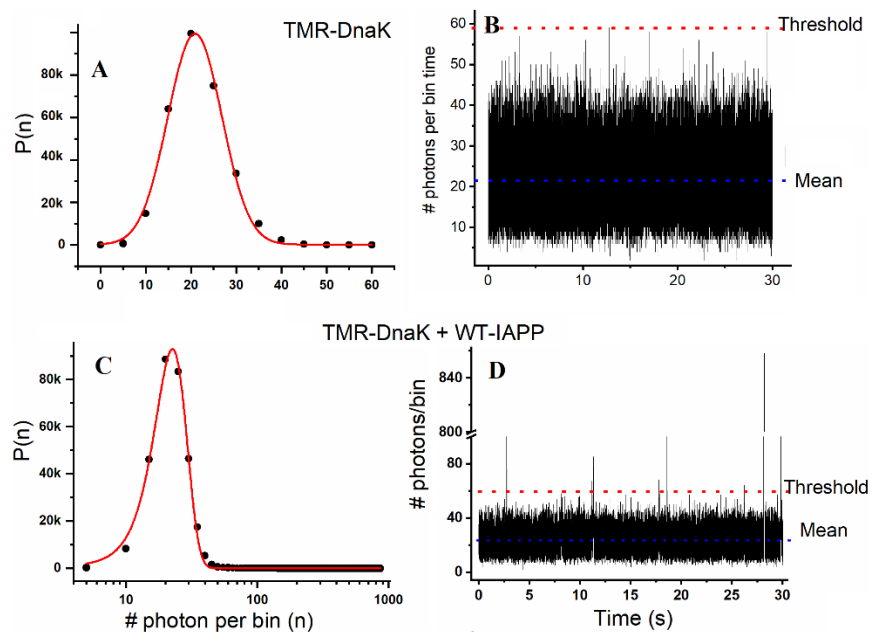
Supplementary Figure S1: Mass spectrometry of chemically synthesized purified IAPP. Molecular weight (MW) and the purity of the chemically synthesized IAPP were confirmed by mass spectrometry. The MW of IAPP was measured to be 3904.9 Da, which is same as the theoretical MW of IAPP containing disulphide bridge between cysteines placed at position 2 and 7. MW of the peaks placed on the right side of the main peak are 3925.2 and 3949.2 Da. These peaks are corresponding to the sodium adducts of IAPP.



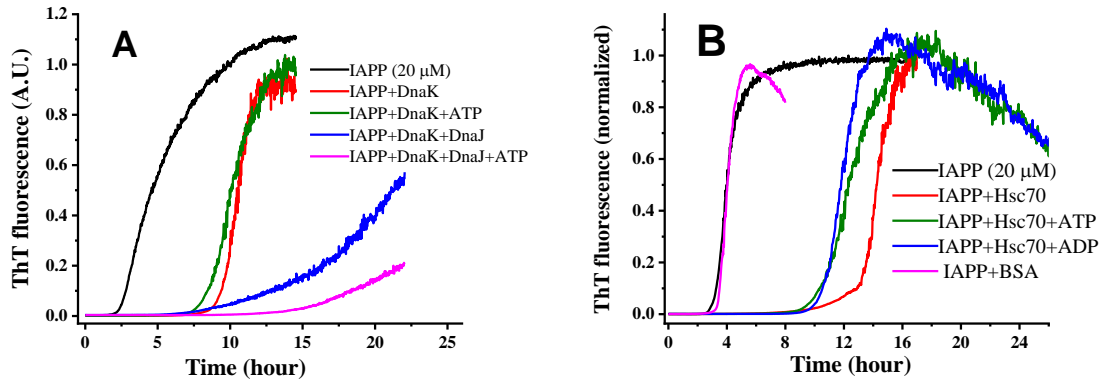
Supplementary Figure S2: SDS-PAGE of purified *E. coli* DnaK, MTB-Hsp70 and human Hsc70. A single dominant band indicates that the proteins are considerably pure.

Burst detection and estimation

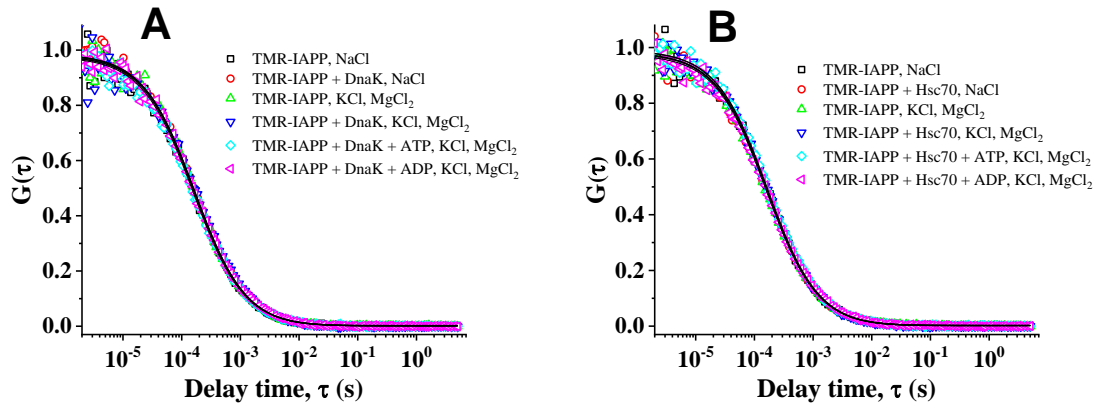
As mentioned in the main text quantitative estimation of photon bursts in presence of large background fluorescence arising due to monomeric TMR-DnaK is difficult. Hence, we have tried to provide a qualitative estimation of the frequency and brightness of the bursts obtained from sample containing 100 nM TMR-DnaK in presence of 20 μ M IAPP. Here we show a representative example. Supplementary Figure S3A and C show the photon counting histogram (PCH) data that are fit with a Gaussian function. The mean and the SD obtained from the fit in A and C are 20 and 13 photons per bin time. The bin time here is 100 μ s. Figure S3B and D show the raw photon count trace collected over 30 seconds. The blue dotted line and red dotted lines represent the mean and threshold (threshold = mean + 3 \times SD = 59 photons per bin time). The threshold is chosen such that frequency of bursts detected in the control sample, i.e., in 100 nM TMR-DnaK is nearly zero. The peaks are extracted from the photon counts data using Mathematica.



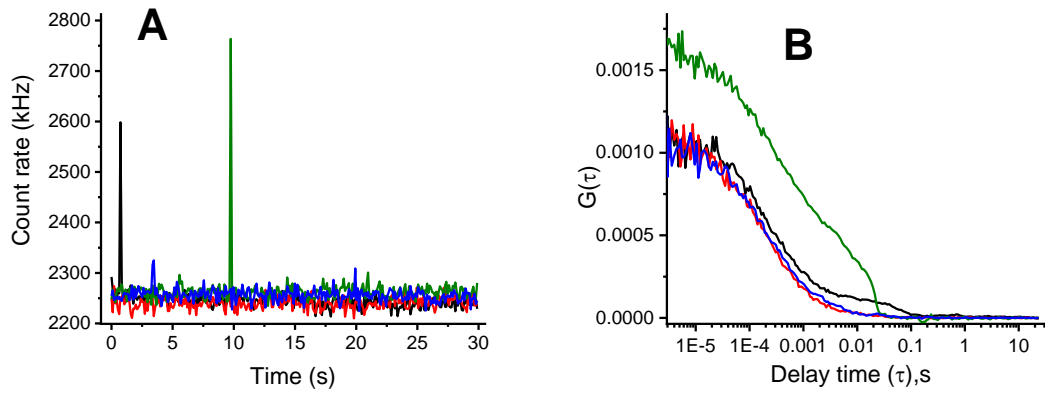
Supplementary Figure S3. Choosing a threshold for detection of photon bursts. Photon counting histogram data obtained from 100 nM TMR-DnaK in absence (A) and in presence of 20 μ M IAPP (C). The PCH data are fit using a gaussian function. The mean and the SD obtained are nearly same in both cases. The threshold for peak detection is set at mean + 3 \times SD = 59 photons per bin time. The bin time here is 100 μ s. How the threshold works to choose the bursts are shown in B and D. From D it is clear that TMR-DnaK exhibits several bursts above the threshold in presence of IAPP.



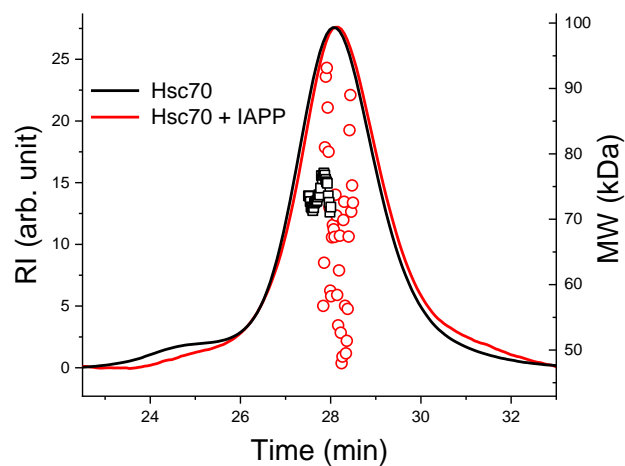
Supplementary Figure S4. Effect of DnaK (A) and Hsc70 (B) on aggregation of IAPP under various solution conditions. Concentrations of IAPP used is 20 μ M. Concentration of Hsc70, DnaK and DnaJ used is 80 nM. All the experiments are performed in 10 mM phosphate buffer at pH 7.4 in presence of 2 mM sodium azide, 5 mM $MgCl_2$ and 100 mM KCl. The ATP dependent experiments are performed in presence of 2 mM ATP. The aggregation is monitored continuously using fluorescence of thioflavin T. The samples are stirred continuously using Teflon coated magnetic micro beads at 37 $^{\circ}C$. It may be observed that both DnaK and Hsc70 strongly delay aggregation of IAPP even at low substoichiometric concentration (1:250 molar ratio) under all of the solution conditions tested here. The inhibitory effect is enhanced further in presence of DnaJ and ATP.



Supplementary Figure S5. The autocorrelation data obtained from solutions of 110 nM TMR-IAPP incubated with 1 μ M DnaK (A) or Hsc70 (B) under various solution conditions. The symbols represent data and solid lines are fits with one component diffusion model. The concentration of ATP used is 2 mM. The solutions are prepared in 10 mM phosphate pH 7.4 buffer at pH 7.4. Concentrations of NaCl, KCl, MgCl₂ and ATP used are 150 mM, 100 mM, 5 mM and 2 mM respectively. It may be seen here that the autocorrelation curves obtained under the different conditions are nearly the same, and are identical to free TMR-IAPP. Therefore, the FCS measurements indicate that most of TMR-IAPP in these solutions are free.



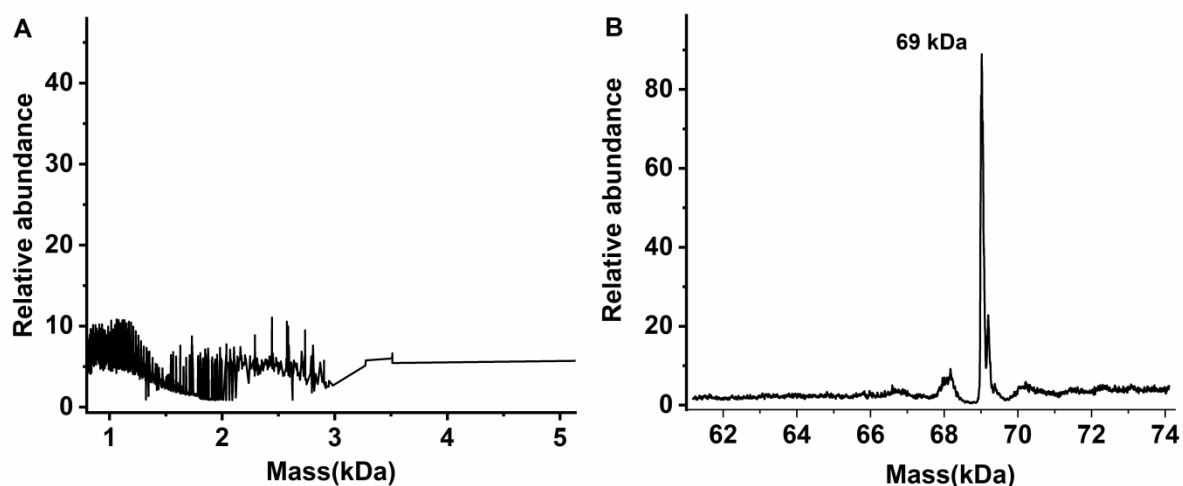
Supplementary Figure S6: Heterogeneity of the TMR-IAPP solution observed in FCS. Four representative photon count traces (A) and autocorrelation curves (B) obtained from FCS measurement of a 400 nM TMR-IAPP solution. A photon count trace and the corresponding autocorrelation trace are shown in the same color. The photon bursts in (A) indicate presence of oligomers in the solution. Presence of photon burst is seen to distort the shape of the corresponding autocorrelation trace (see the black and the blue traces).



Supplementary Figure S7. SEC-MALS measurement of Hsc70 incubated with or without IAPP. The concentrations of Hsc70 and IAPP used are 5 and 20 μM respectively. The solid lines represent concentrations of the protein measured using refractive index (RI). The symbols represent molecular weight (MW) of the peak fraction measured using multiangle light scattering. It may be seen that both the RI profile and values of MW do not change significantly in presence of IAPP. The theoretical MW of Hsc70 is 71 kDa.

Mass spectrometry of the TMR-IAPP/DnaK solution following fractionation by Size exclusion Chromatography

TMR-IAPP/DnaK complexes were fractionated using size exclusion chromatography (SEC), which is coupled to the multiangle light scattering (MALS) setup. The fraction exhibiting the highest peak in the refractive index (RI) detector was collected for mass spectrometry measurements. Mass spectrometry measurements were performed using a 6545 Q-TOF ESI-MS (Agilent technologies). The spectrometer is coupled to a HPLC for desalting of the injected sample. The m/z spectra were deconvoluted with the MassHunter software (Agilent, UK) using the resolved isotope deconvolution method for measuring the mass of peptides ($MW < 10$ kDa), and the maximum entropy deconvolution method for measuring the mass of proteins ($MW > 10$ kDa).



Supplementary Figure S8: Mass spectrometry of the TMR-IAPP/DnaK sample following fractionation by SEC. A) Deconvolution of the m/z spectra of IAPP was performed within a mass range of 0 to 5000 Da using the resolved isotope method. Deconvolution within this mass range did not detect any IAPP, indicating that concentration of IAPP in the SEC fraction must be very low. B) Detection of DnaK by deconvolution of m/z spectrum within a mass range of 60 to 80 kDa. Presence of DnaK (69 kDa) is quite clear. Hence, the SEC purified fraction contains primarily free DnaK and possibly a very low concentration of the complexes.

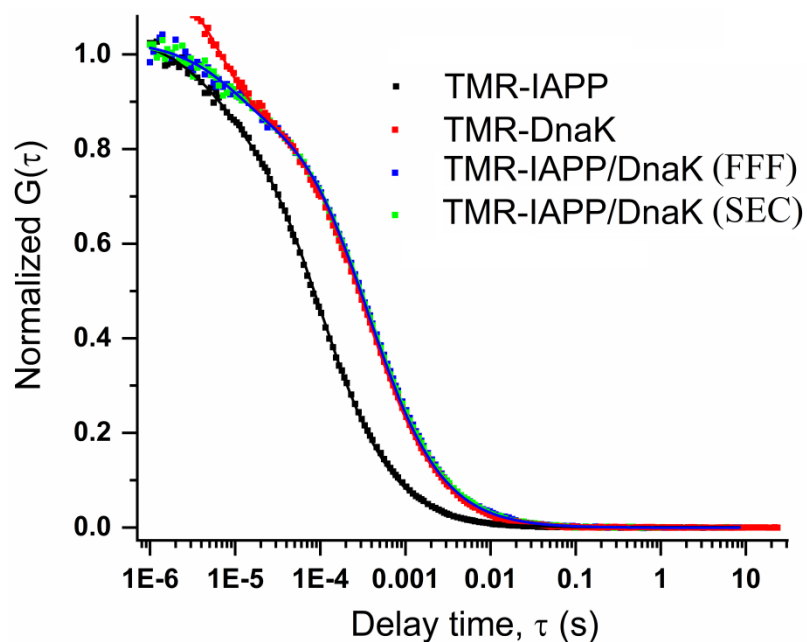
Autocorrelation data $G(\tau)$ obtained from the FCS measurements of SEC or FFF purified TMR-IAPP/DnaK

FCS measurements were performed on free rhodamine B, TMR-IAPP, TMR-DnaK and SEC or FFF purified fractions of TMR-IAPP/DnaK solution. Free rhodamine B (50 nM) was used as a control to characterize the FCS observation volume. TMR-IAPP (50 nM) and TMR-DnaK (50 nM) were used to estimate the hydrodynamic radii (R_h) of these proteins in the unbound monomeric forms. The major fractions of the SEC or FFF purified TMR-IAPP/DnaK solution was used directly for FCS measurements. The FCS data were analysed using a single diffusion and single relaxation model (1) (see supplementary eq. S1). The relaxation component was used to take care of the contributions from conformational fluctuations and/or the triplet state dynamics. Concentrations of the purified samples were determined from the $G(0)$ of the autocorrelation data..

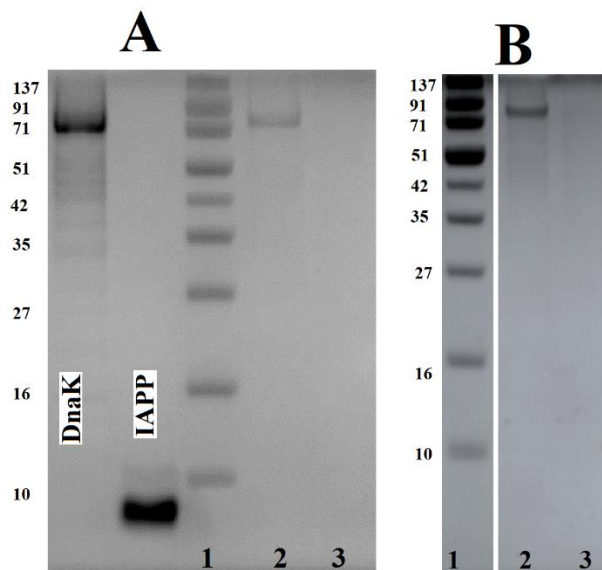
$$G(\tau) = \frac{1}{\langle N \rangle} \left(\frac{1 - F_R + F_R \text{Exp}\left(-\frac{\tau}{\tau_R}\right)}{1 - F_R} \right) \frac{1}{\left(1 + \frac{\tau}{\tau_D}\right) \left(1 + \frac{\tau}{\omega^2 \tau_D}\right)^{0.5}} \quad (\text{eq. S1})$$

Here $\langle N \rangle$ is average number of molecules in the FCS observation volume. F_R and τ_R are the relative amplitude and the characteristic time of the relaxation component respectively. The τ_D is the diffusion time of the molecule and ω is the axial ratio of the FCS observation volume. It may noted here that $\langle N \rangle^{-1}$ is $G(0) \times (1 - F_R)$. Hence, in absence of the relaxation component $\langle N \rangle^{-1}$ is simply equal to $G(0)$. Hydrodynamic radius (R_h) of the proteins are estimated from the measured diffusion times using the following relationship (see eq. S2). The R_h of rhodamine B used is 0.57 nm².

$$R_{h,protein} = \frac{\tau_{D,protein}}{\tau_{D,rhodamineB}} R_{h,rhodamineB} \quad (\text{eq. S2})$$



Supplementary Figure S9: Normalized autocorrelation data $G(\tau)$ obtained from FCS measurements of SEC or FFF purified IAPP/DnaK. TMR-IAPP (black), TMR-DnaK (red), SEC purified fraction (green) or FFF purified fraction (blue) of the TMR-IAPP/DnaK sample in PBS, pH 7.4 buffer at RT. For SEC or FFF purified samples, the fractions exhibiting the highest RI were taken for the FCS measurements. The symbols represent data and the solid lines were fit using a single diffusion and single relaxation model (see supplementary eq. S1). The diffusion time (τ_D) was used for estimation of the hydrodynamic radius of the molecules (see supplementary eq. S2).



Supplementary Figure S10: SDS-PAGE of the SEC fractions of atto425-DnaK/TMR-IAPP solution. Gels stained by either Coomassie Brilliant Blue staining solution (A) or by silver staining (B). In both A and B, the lane 1 shows the standard markers with molecular weights noted in kDa in the left side of the respective gels. Lanes 2 and 3 represent SEC fractions eluted at 28 and 17 minutes respectively (see Figure 7 in the main manuscript). It may be noted that the fraction eluted at 28 min exhibits a peak in the SEC. The MW corresponding to the peak is about 70 kDa, which is equal to the MW of DnaK. No protein is detected in the fraction eluted at 17 min (see lane 3) indicating very low concentration of proteins in this fraction. In figure A, the first two lanes represent purified 10 μ M atto425-DnaK and TMR-IAPP respectively. In B, although all the lanes are part of the same gel, the image has been edited to move the lane 1 in the lateral direction to bring it closer to lanes 2 and 3.

A 500 μ l solution of 2 μ M atto425 labeled -DnaK and 4 μ M TMR-labeled IAPP was incubated O/N at 25 $^{\circ}$ C. The solution is then fractionated by size exclusion chromatography (SEC) using a Superdex 200 column (GE Healthcare, USA). The running buffer used is PBS at pH 7.4. The chromatogram is shown in Figure 7 in the main manuscript. An aliquot of 20 μ l of sample is collected for SDS-PAGE. The gel used is a 12 % polyacrylamide gel. The SDS-PAGE is performed at 200 volts for about 35 minutes. The gels are stained using Coomassie Brilliant Blue staining solution or by silver staining as mentioned above using standard protocols.

Supplementary Table S1: Summary of the parameters obtained from fitting of the FCS data

Sample	$\langle N \rangle$	τ_D (μ s)	F	τ_R (μ s)	Conc. (nM)	R_h (nm)
TMR-IAPP	22 \pm 2	119 \pm 2	0 (fixed)*	NA	20	1.2
TMR-DnaK	55 \pm 2	398 \pm 4	0.2 \pm 0.001	14 \pm 1	50	3.3
TMR- IAPP/DnaK (from FFF)	16 \pm 3	397 \pm 20	0.1 \pm 0.004	15 \pm 1	15	3.3
TMR- IAPP/DnaK (from SEC)	50 \pm 5	385 \pm 20	0.09 \pm 0.003	15 \pm 1	45	3.3

The abbreviations $\langle N \rangle$, τ_D , F and τ_R have usual meaning as described in supplementary eq. S1. Concentration is calculated from $\langle N \rangle$. In our setup we find $\langle N \rangle / \text{Conc.} = 1.1 / \text{nM}$. Calibration of the FCS observation volume is performed using rhodamine B solutions (2). The hydrodynamic radius (R_h) is estimated using supplementary eq. S2.

*In case of TMR-IAPP the value to F was set to 0.0 to avoid redundancy in the values of the fitting parameters.

References

1. Sil, T. B., Sahoo, B., and Garai, K. 2018. Building, Characterization, and Applications of Cuvette-FCS in Denaturant-Induced Expansion of Globular and Disordered Proteins. *Methods in enzymology* 611:383-421.
2. Sahoo, B., Sil, T. B., Karmakar, B., and Garai, K. 2018. A Fluorescence Correlation Spectrometer for Measurements in Cuvettes. *Biophysical journal* 115:455-466.